

1 The mechanism of Peony Seed Oil can promote sleep by 16S  
2 rRNA gene sequencing and metabolomics analyses of changes  
3 in the intestinal flora and biomarkers in mice

4 Ziyue Liang, Junjie Zhang, Zhiyuan Wang, Xinyi Li

5 <sup>1</sup>College of Agriculture/Tree Peony, Henan University of Science and Technology, Luoyang,  
6 471023, China

7

8 **Abstract:**

9 Peony seed oil (PSO) is an edible oil rich in unsaturated fatty acids. Experimental  
10 results show that PSO can be a safe edible oil with sleep-improving effects. We used  
11 untargeted metabolomics and 16S rRNA amplicon sequencing to analyze the  
12 mechanism by which PSO improves sleep. The results showed that PSO improves sleep  
13 by modulating the gut microbiota. Additionally, PSO altered gut metabolites, with some  
14 of these metabolites involved in sleep regulation. These results demonstrated that long-  
15 term dietary PSO plays beneficial roles in sleep by modulating the gut bacteria and gut  
16 metabolism in mice.

17 **Keywords:** peony seed oil; Sleep; Metabolomics; Gut microbiota; 16S rRNA

18

19

20

21

22

23

24

25

26

27

28

29 **Introduction**

30 Sleep is an extremely important physiological function to maintain human life,  
31 which is essential to human body. With the fast pace of today's society and people's  
32 working stress increases, 15–35% of adults suffer from regular sleep disruptions, such  
33 as difficulties in initiating sleep, insufficient sleep time or frequent waking during the  
34 night<sup>[1]</sup>. Sleep problems is often caused by long-term mental burden, mental work, weak  
35 after illness and other causes<sup>[2]</sup>. Sleep problems will damage people's daytime lives by  
36 feeling exhausted and making troubles. Moreover, persistent sleep problems are  
37 frequently associated with cardiovascular diseases, obesity, diabetes, and mortality<sup>[3]</sup>.

38 With the popularization of nutrition knowledge, people's awareness of food, drugs  
39 and nutrition has been significantly improved, and more and more attention has been  
40 paid to the relationship between diet and health. At present, the research on functional  
41 oils is one of the active functional food research fields in the world, which mainly  
42 studies the functional role of unsaturated fatty acids<sup>[4,5]</sup>. It is found that polyunsaturated  
43 fatty acids are of great significance in biology and nutrition<sup>[6,7]</sup>.

44 Recent studies indicate that alterations in the gut microbiota might be associated  
45 with sleep through the gut–brain axis<sup>[8]</sup>. Anderson et al. found that better sleep quality  
46 was connected with higher proportions of the gut microbial phyla Verrucomicrobia and  
47 Lentisphaerae in healthy adults, suggesting a possible relationship between sleep  
48 quality and the gut microbiota<sup>[9]</sup>. Poroyko et al. showed that chronic sleep  
49 fragmentation (SF) was related to the gut microbiota through conventionalization of  
50 germ-free mice with the gut microbiota of mice<sup>[10]</sup>.

51 Peony seed oil contained in the human body needs of polysaccharide, vitamin E,  
52 trace elements, and contains a lot of unsaturated fatty acid, which have the potential  
53 function of anti-oxidation, auxiliary treatment of diabetes, enhance immunity, anti-  
54 inflammation<sup>[11]</sup>. In China, the current development of peony seed oil is in the stage of  
55 vigorous development. The content of unsaturated fatty acids in peony seed oil reached  
56 more than 90%<sup>[12]</sup>. To carry out the study of peony seed oil related active functions for  
57 the development of peony seed oil related drugs, health products and high-end edible  
58 oil to provide a theoretical basis. At the same time, it is significance to promote national

59 health and improve economic benefits.

60 This study aims to investigate the effect of PSO administration on intestinal flora  
61 and biomarkers in mice and to explore the potential linkage. To this end, we probed the  
62 changes in gut microbiota and intestinal biomarkers after PSO administration and  
63 investigated the possible links between them. The differences in gut microbial  
64 community structure and gut metabolomics were analyzed by 16S rRNA sequencing  
65 technology and LC/MS analysis, respectively. In this work, we (1) compared the  
66 composition of peony seed oil with commonly used peanut oil and soybean oil through  
67 gas chromatography-mass spectrometry analysis. (2) Established an animal model to  
68 observe the regulatory effect of peony seed oil on sleep in mice, and measured blood  
69 markers and liver tissue sections to determine the impact of the three oils on the growth  
70 process of mice. (3) Analyzed the regulatory effect of peony seed oil on the gut  
71 microbiota of mice using 16S rDNA amplicon diversity sequencing. (4) Conducted  
72 metabolomics analysis to examine the effects of peony seed oil on mouse feces, and  
73 performed integrated omics analysis to reveal the mechanism by which peony seed oil  
74 regulates sleep in mice.

## 75 **2 Materials and Methods**

### 76 2.1 Determination of unsaturated fatty acids in peony seed oil, peanut oil and soybean 77 oil

78 This experimental method is based on previous article<sup>[13]</sup>.

### 79 **2.2 Animal ethics statement**

80 Fifty SPF grade male ICR mice, which were aged 5-6 weeks (30 g). They were  
81 purchased from Henan SKobes Biotechnology Co., LTD (Henan, China; License  
82 number SCXK2020-0005). The room temperature range was kept at  $25 \pm 2^{\circ}\text{C}$  and the  
83 humidity was maintained at  $40\% \pm 5\%$ . In addition, the 12-hour light-dark cycle, the  
84 clean bedding, and unrestricted access to both water and standard dry pellet feed. All  
85 protocols in this study were approved by the Animal Experiment Committee of Henan  
86 University of Science and Technology (No. 20190719016).

### 87 **2.3 Animal grouping and treatment**

88 After 1 week of feeding, the mice were randomly divided into 4 groups with 5 mice  
89 in each group. The groups included the control group (Con group) at a dosage of 0.5  
90 mL normal saline + basal diet. The peony seed oil group (PSO group) at a dosage of  
91 0.5 mL oil + basal diet. The peanut oil group (PNO group) at a dosage of 0.5 mL oil +  
92 basal diet, the soybean oil group (SBO group) at a dosage of 0.5 mL oil + basal diet.  
93 The basal diet consists of 9% water, 18% to 22% protein, 4% fat, 5% fiber, 8% ash, and  
94 52% to 56% nitrogen-free extract.

## 95 **2.4 Collection and processing of experimental animal samples**

96 Mouse feces were collected on the last day of the assay for gut microbiome and  
97 metabolomics analysis. In addition, the heart was punctured to take blood, serum was  
98 taken, and the heart was separated at 3000 rpm for 15 minutes. Livers were collected  
99 from sacrificed mice for biochemical analysis. Serum total cholesterol (TC),  
100 triglyceride (TG), high-density lipoprotein cholesterol (HDL-C) and low-density  
101 lipoprotein cholesterol (LDL-C) and glucose (Glu) were analyzed by commercial  
102 diagnostic kits (Solarbio, China).

## 103 **2.5 Histological observation of liver tissues**

104 Liver tissues were soaked 1 cm × 1 cm in 4% paraformaldehyde at 4 °C for 24 hours,  
105 and gradient dehydration was carried out with ethanol of different concentration  
106 gradients. Then the liver tissue was treated with xylene to make it transparent. Then the  
107 wax was dipped with paraffin wax to control the xylene. The liver tissue after wax  
108 immersion was embedded by embedding machine, and bubbles and cracks were  
109 avoided as much as possible during the embedding process. Then the slices were sliced  
110 and sealed with neutral gum. The sealed slices were placed under a microscope for  
111 examination and image acquisition and analysis.

## 112 **2.6 Sleep assays**

### 113 **2.6.1 Direct sleep test**

114 The mice were given continuous intragastric administration 12 weeks, and the  
115 number of sleeping mice in each group was observed after the last oil administration.  
116 Sleep is marked by the disappearance of the righting reflex, that is, when the mouse is

117 placed in the back horizontal position, those who cannot righting for more than 1 min  
118 are regarded as asleep.

### 119 **2.6.2 Prolonged sleep time in mice induced by pentobarbital sodium**

120 Mice in each group were given intraperitoneal injection of pentobarbital sodium at  
121 41mg/kgbw dose (0.1mL/10gbw) 15 min after the last administration of the test  
122 substance. The sleep duration of pentobarbital sodium was recorded after the reversal  
123 reflex disappeared for more than 1 min as the criterion for sleep.

### 124 **2.6.3 Sodium barbiturate sleep latency test**

125 Mice were given continuous intragastric administration for 12 weeks, and then  
126 intraperitoneally injected barbiturate sodium at the dose of 295 mg/kgbw  
127 (0.1mL/10gbw) 15 min after the last administration. The sleep latency time of each  
128 group of mice was recorded with the disappearance of righting reflex for 1 min as the  
129 index of sleep.

### 130 **2.6.4 Pentobarbital sodium subthreshold dose hypnosis experiment**

131 Mice were given continuous intragastric administration for 12 weeks, and  
132 pentobarbital sodium was intraperitoneally injected into each group at a dose of  
133 32mg/kgbw, the injection amount was 0.1mL/10gbw, and the elimination of righting  
134 reflex for more than 1 minute was taken as the sleep index, and whether the mice in  
135 each group fell asleep was recorded.

## 136 **2.7 Gut microbiota analysis**

137 The analysis of the composition of the gut flora involves the extraction of total  
138 genomic DNA from the sample. DNA purity was determined on 1% agarose gel and  
139 the concentration was adjusted to 1 ng/ $\mu$ L with sterile water. Then, after designing the  
140 conserved primers and performing PCR amplification, the sequencing adapter was  
141 connected to the end of the primers. Sequencing libraries were prepared with purified  
142 PCR products.

143 The raw readings obtained by sequencing were percolated using Trimmomatic v 0.33  
144 software. Usearch v10 software was used to merge clean reads of each sample, and the  
145 length of the combined data was permeated according to the length range corresponding  
146 to different regions. The chimeric sequences were detected and removed using

147 UCHIME v4.2 software to obtain the final set of valid reads. Usearch software was  
148 used to cluster the sequences, the similarity threshold was 97.0%, and the operation  
149 classification unit (OTU) was obtained. SILVA is used as reference database for  
150 classification and annotation of feature sequences. QIIME 2 software (v 1.8.0) was used  
151 to select the sequences with the most abundant features at the phylum and genus  
152 classification level as representative sequences. The  $\alpha$ -diversity and  $\beta$ -diversity  
153 indices of the samples were evaluated by QIIME 2.

## 154 **2.8 Untargeted metabolomics analysis of faeces**

155 Fecal metabolites were separated employing a triple TOF-6600 mass spectrometer  
156 (AB Sciex, USA) and LC20 ultra-high performance liquid chromatography (UPLC) on  
157 a Waters ACQUITY UPLC HSS T3 C18 column (100 mm  $\times$  2.1 mm, 1.8  $\mu$ m,  
158 Shimadzu, USA). The column temperature was 40°C and the sample size was 2  $\mu$ L.  
159 The mobile phase included ultra-pure water in phase A (containing 0.1% formic acid)  
160 and acetonitrile in phase B (containing 0.1% formic acid) at a flow rate of 0.4 mL/min.  
161 Positive mode: mobile phase A: 0.1% formic acid, mobile phase B: methanol; Negative  
162 mode: mobile phase A: 5 mM ammonium acetate, pH 9.0, mobile phase B: methanol.  
163 The gradient elution conditions were set as follows: 0 min: 98% A phase, 2% B phase;  
164 1.5 min: 98% phase A, 2% phase B; 3 min: 15% phase A, 85% phase B; 10 min: 0% A  
165 phase, 100% B phase; 10.1 min: 98% phase A, 2% phase B; 11 min: 98% phase A, 2%  
166 phase B; 12 min: 98% phase A, 2% phase B.

167 During LC-MS/MS analysis, positive and negative data are imported into the  
168 MetaboAnalyst R package (v 3.1.3). Secondly, partial least squares discriminant  
169 analysis (PLS-DA) and orthogonal partial least squares discriminant analysis (OPLS-  
170 DA) were used to visualize the metabolic differences among the groups. fold change  
171 (FC) method was used to determine the metabolite change amplitude, combined with *P*  
172 value, and the metabolites with significant differences between groups were screened.

## 173 **2.9 Integrative analysis**

174 Spearman correlation analysis was conducted between intestinal metabolites and  
175 serum indexes in the top 20 abundance and intestinal microorganisms in the top 20

176 abundance, and *P*-values were obtained, which were visually displayed using heat maps.

## 177 **2.10 Statistical analysis**

178 SPSS software v 22.0 (SPSS, Inc., Chicago, IL, USA) was used for statistical analysis.  
179 One-way ANOVA and least significant difference (LSD) multiple comparison tests  
180 were used for comparison between groups. The results were plotted using OriginPro  
181 2024b Learning Edition.

## 182 **3. Results**

### 183 **3.1 Determination of unsaturated fatty acid composition of PSO, PNO and SBO**

184 We used GC-MS to determine unsaturated fatty acid composition of different oils.  
185 They are mainly oleic acid, linoleic acid, linolenic acid. Among them, the content of  
186 unsaturated fatty acid in PSO was 91.99% in total (Figure S1, Supplementary Table 1).  
187 PNO' unsaturated fatty acid content was 54.02% (Figure S2, Supplementary Table 2).  
188 The percentage composition of unsaturated fatty acid of SBO was 63.37% (Figure S3,  
189 Supplementary Table 3). These results showed that PSO had the rich unsaturated fatty  
190 acid.

### 191 **3.2 Effects of the long-term intake of PSO on the physiological status of mice.**

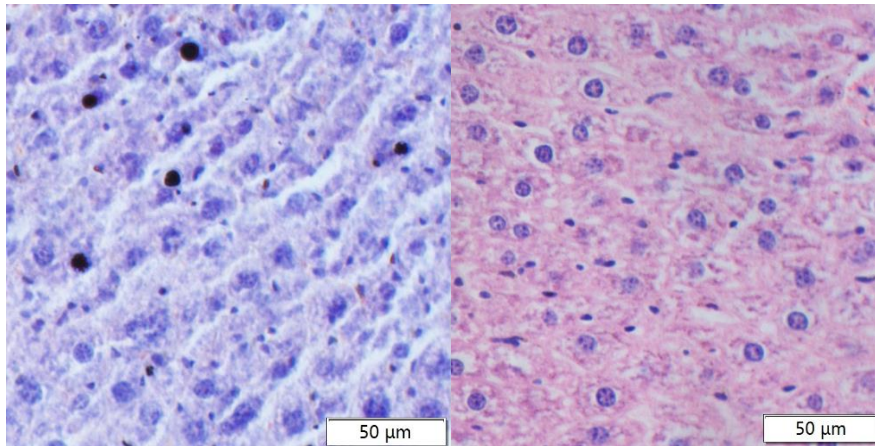
192 Hematoxylin and eosin (H&E) staining method was employed to observe liver  
193 tissues morphology of mice after dietary PSO for 12 weeks. In Figure 1A-D, we can  
194 clearly see that after the three kinds of oil were fed to mice, compared with the Con  
195 group, the tissue cells of the liver sections were uniform, closely arranged, with dense  
196 nuclei and no fat particles, indicating that there was no difference in food safety  
197 between peony seed oil and the other two common edible oils.

198 Lack of sleep can affect lipid metabolism and lead to elevated blood lipid levels. We  
199 used PSO, PNO and SBO to gavage treatment in different group mice. As shown in  
200 Figure 2, the level of Glu, TC, TG, HDL-C and LDL-C in PSO group and Con group  
201 had little difference, Also, PSO made the level of HDL-C in mice higher. In addition,  
202 there was also less difference between the PSO, PNO and SBO groups. These results  
203 suggested PSO and other oils for daily consumption have little effect on cholesterol  
204 metabolism.

205

206 A

B

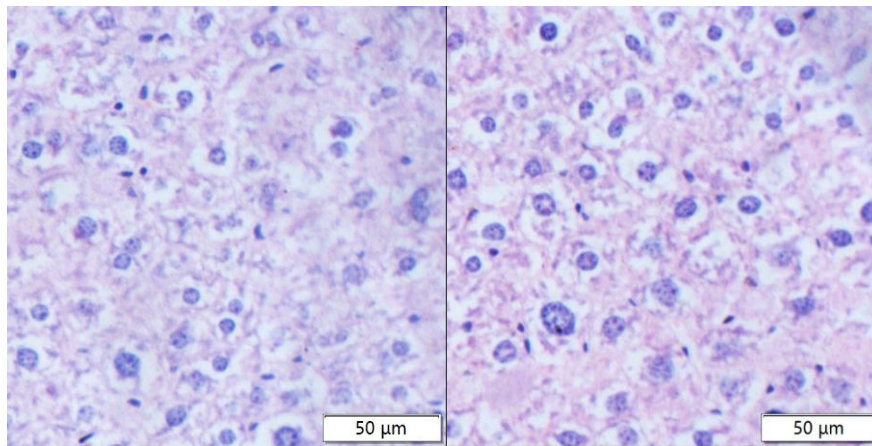


207

208

209 C

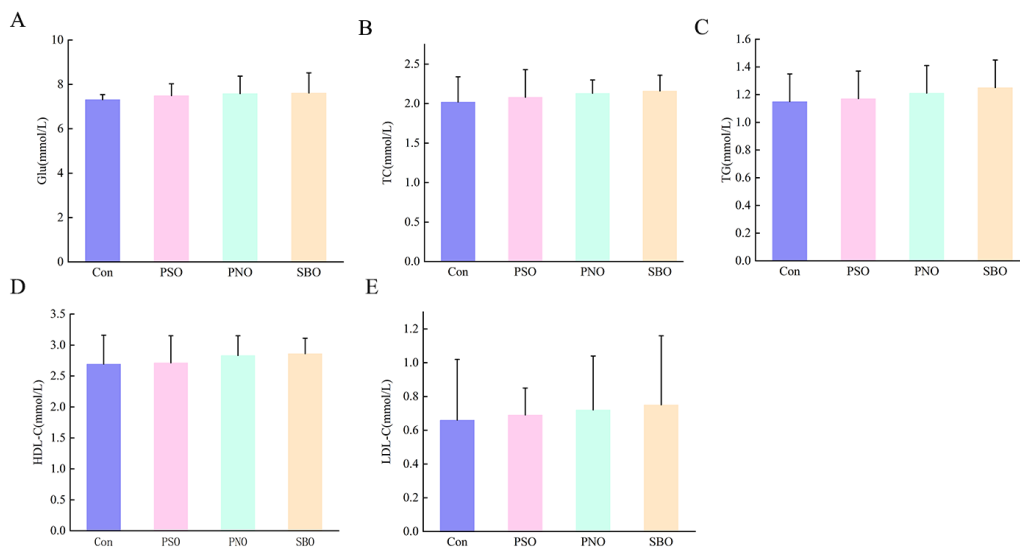
D



210

211 Figure 1. Representative images of hematoxylin and eosin-stained liver tissue for (A)

212 Con group, (B) PSO group, (C) PNO group, (D) SBO group. Scale bar = 50 μm.



213

214 Figure 2 Effect of PSO, PNO and SBO on the levels of Glu (A), TC (B), TG (C), HDL

215 (D), LDL-C (E) in mice. The data were presented as the mean  $\pm$  SEM (n = 10).

216

### 217 3.3 Effects of the long-term intake of PSO on improving sleep function in mice

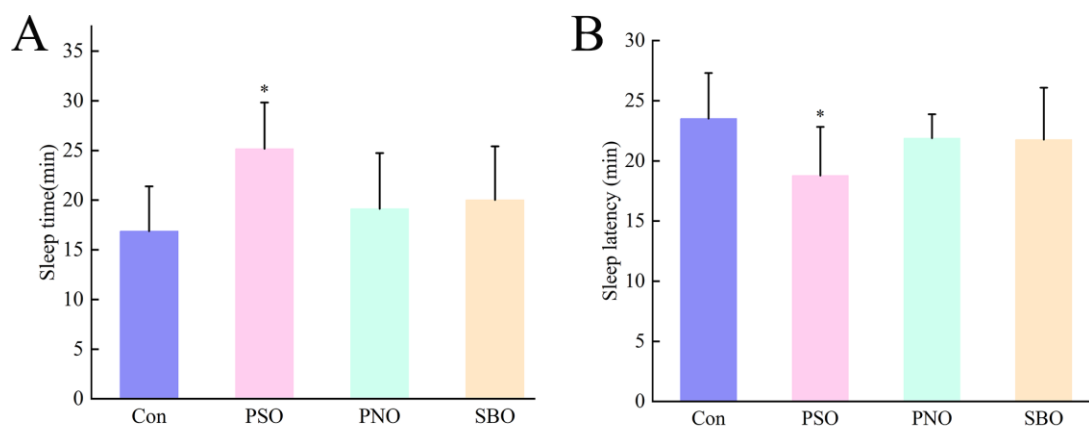
218 Direct sleep test observation found that mice in the peony seed oil group were more  
219 lethargic and had better sleep conditions. Then, the following experiment was  
220 conducted to analyze the sleep conditions of mice in different oil groups through data.

221 As shown in Figure 3A, the sleep time of mice was obviously lengthened in PSO  
222 group when compared with the Con group, and there was statistical difference ( $P <$   
223 0.05). PNO group and SBO group could prolong the sleep time, but they didn't exist  
224 statistical difference. Furthermore, the prolonged rate was 38.4%, 13.3%, 18.6% in PSO  
225 group PNO group and SBO group, respectively.

226 The sleep latency in the PSO group was shorter than that in Con group (Figure 3B),  
227 and the differences were significant ( $P < 0.05$ ). However, though PNO and SBO could  
228 reduce the sleep latency, but not remarkable. What's more, the reduction rate of sleep  
229 latency was 20.1%, 7.4%, 6.9% respectively.

230 After using pentobarbital sodium to treat mice, the result showed that the rate and  
231 the amount of mice in PSO group had great increase compared with Con group (60%).  
232 The rates of falling asleep PNO group and SBO group had markedly increase with 30%  
233 and 50%, respectively (Table 1).

234



235

236 Figure 3 (A) Effect of PSO on the sleep time of mice induced by pentobarbital sodium  
237 in sleep improvement experiment. (B) Effect of PSO on the length of sleep latency in

238 mice induced by barbiturate sodium in sleep improvement experiment. Each bar  
239 represents the mean  $\pm$  SEM (n = 10). \* $P$  < 0.05 vs Con group.

240 Table 1 Effect of PSO on the effects of a subthreshold dose of pentobarbital sodium.

Group	Number of sleeping mice	Rate (%)
Con group	2	20
PSO group	6	60
PNO group	3	30
SBO group	5	50

241

### 242 3.4 Effects of the long-term intake of PSO on the gut microbiota

243 Given that long-term treatment of PSO through diet in direct encounters the intestinal  
244 microbial environment, we next tried to delve the regulation of the gut microbiome by  
245 PSO. We found 6508 OTUs were found in 24 samples based on 97% sequence  
246 similarity (Supplementary Table 4). There are 316 OTUs common to all four groups.  
247 There were 1918, 2599, 800, and 875 OUT in Con group, PSO group, PNO group and  
248 SBO group, respectively (Figure 4A). From the bar chart (Figure 4B), we could see that  
249 the number in PSO group was the most.

#### 250 3.4.1. Analysis of the alpha and beta diversity of the gut microbiota

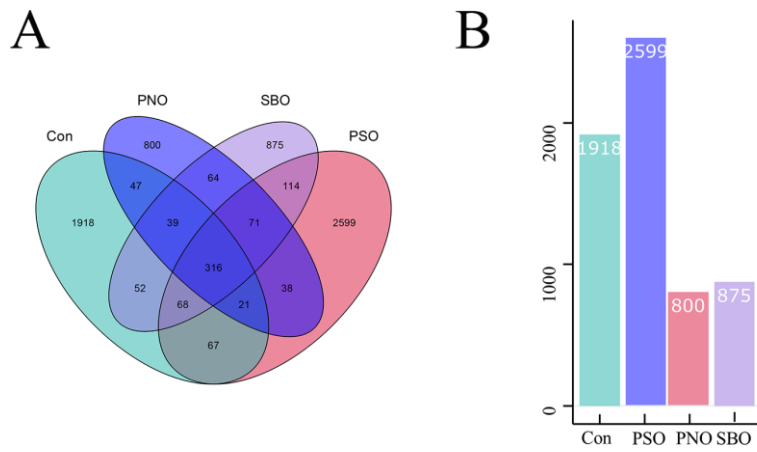
251 Based on alpha diversity analysis, observed features and Chao 1 indexes displayed  
252 that the abundance of PSO group was higher than that of Con group, PNO group and  
253 SBO group (Figure 5A-B). Moreover, Shannon and Simpson indexes demonstrated  
254 there were significant differences in species richness and evenness in PSO group when  
255 compared with Con group (Figure 5C-D,  $P$  < 0.05), but no significant differences  
256 between PNO group and SBO group.

257 Based beta diversity analysis, supervised PLS-DA result showed PSO group and  
258 Con had obvious separation. PNO group and SBO group had a cross aggregation. And  
259 PSO group had significant separation trend compared to PNO group and SBO group as  
260 well (Figure 5E). Principal coordinate analysis (PCoA) of Bray-Curtis distance showed  
261 significant separation between peony seed oil group and blank group. In addition, we

262 observed that the cross-clustering between the peony seed oil group, peanut oil group  
263 and soybean oil group was not obvious (Figure 5F). In short, our study demonstrated  
264 that PSO altered the abundance and diversity of intestinal flora in mice.

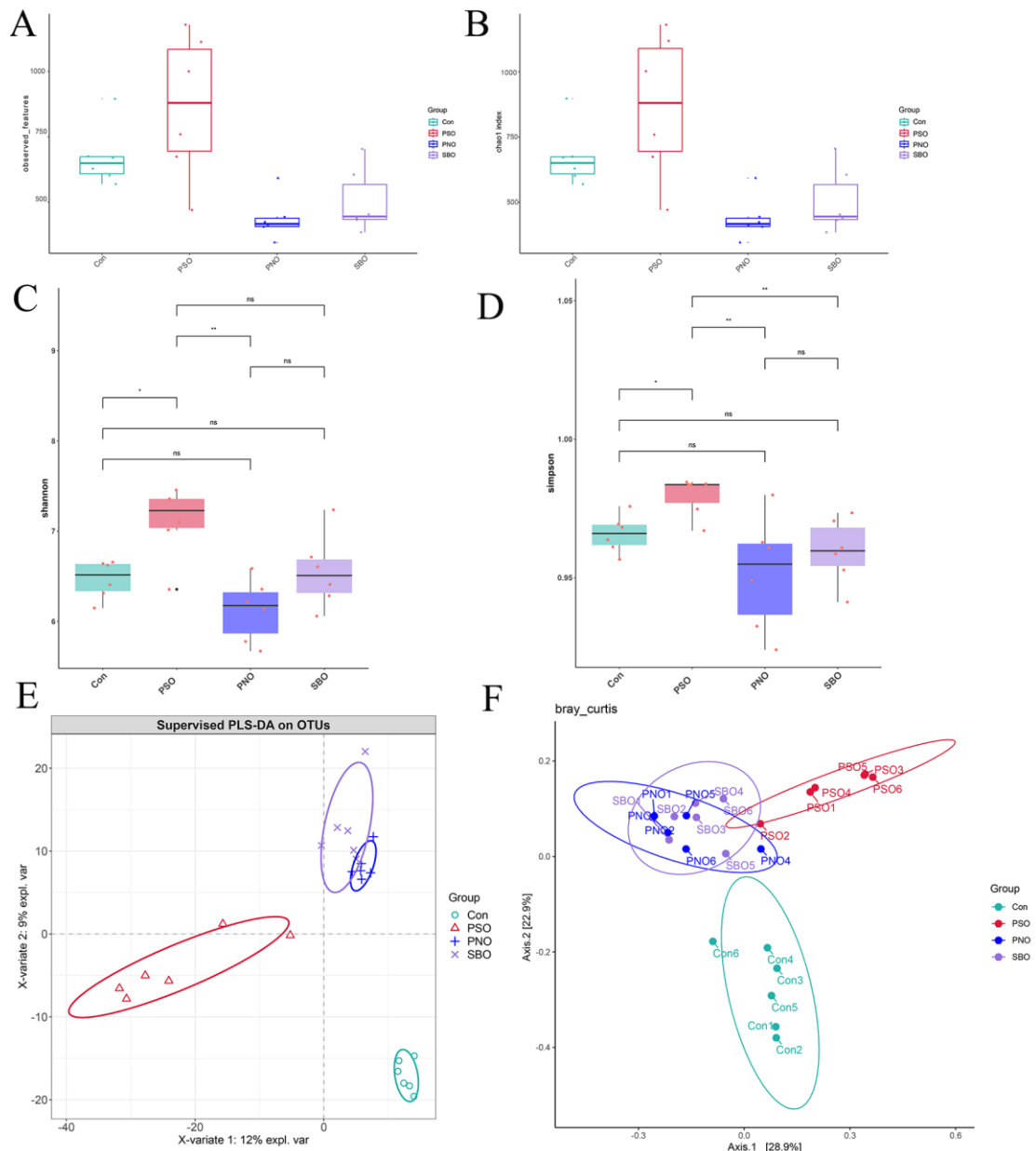
265

266



267

268 Figure 4 (A) Venn diagram for 4 groups. (B) Bar chart of OTUs for 4 groups.



269

270

271 Figure 5 Alpha and beta diversity of gut microbiota among different groups of mice.

272 (A–D)  $\alpha$ -diversity indices of the gut microbiota. (A) observed features index, (B) Chao1

273 index, (C) Shannon index, (D) Simpson's index. (E–F)  $\beta$ -diversity of the gut microbiota.

274 (E) PLS-DA analysis. (F) PCoA analysis of the Bray-Curtis distance based on OTUs.

275 ns: no significant difference, \* $P < 0.05$

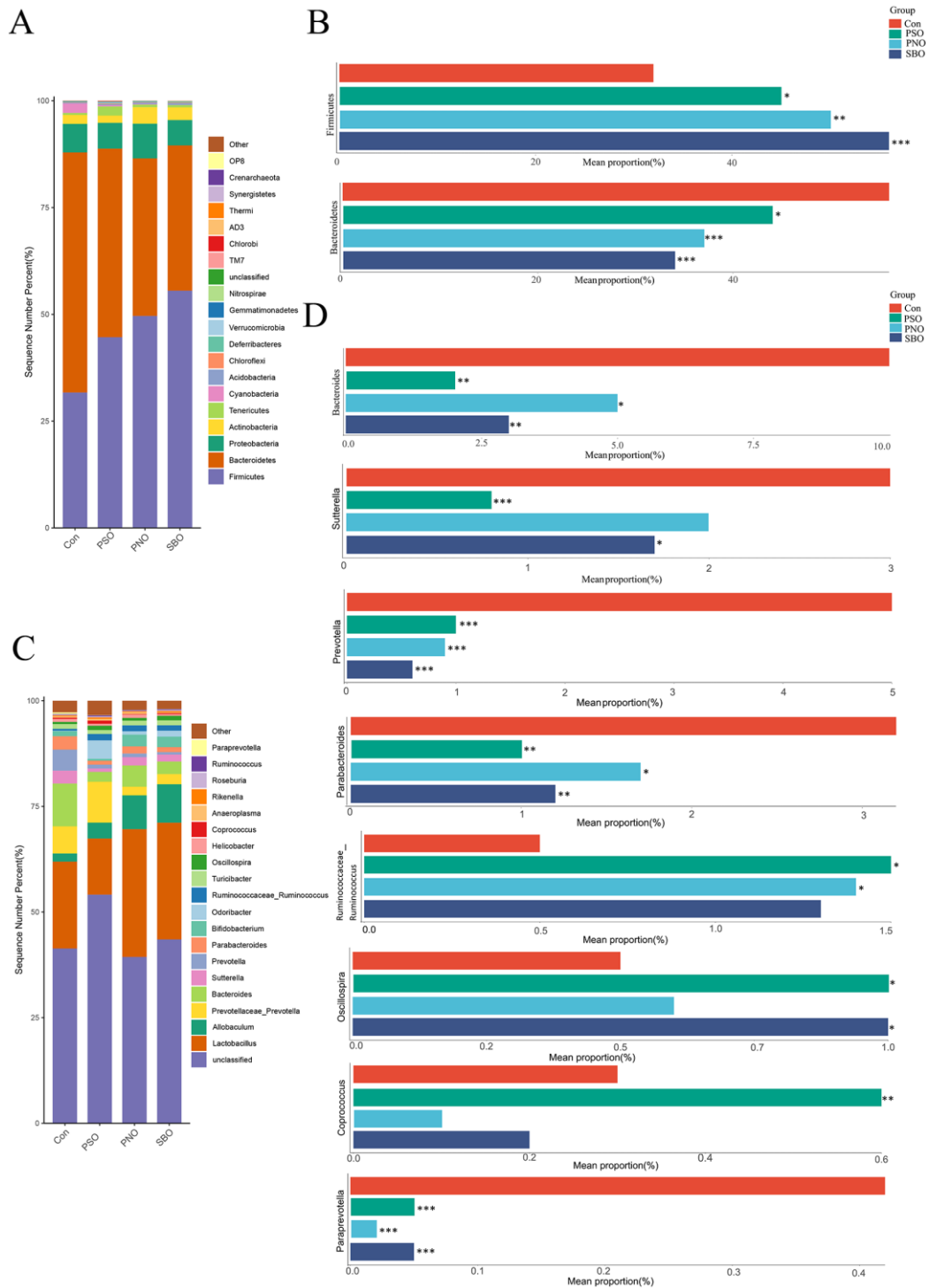
276

277 **3.4.2. Analysis of gut microbiota composition**

278 We analyzed the classification and distribution of microbial composition in Con

279 group, PSO group, PNO group and SBO group. In Figure 6A, At the phylum level, the  
280 composition of top 20 gut microbes manifested that Bacteroidetes was the dominant  
281 bacteria in the Con group, followed by Firmicutes and Proteobacteria, which accounted  
282 for 56.20%. 31.68% and 6.69%. The top 3 predominant bacteria in PSO group are  
283 Firmicutes, Bacteroidetes and Proteobacteria, accounting for 44.64%, 44.15% and 6.03%  
284 respectively. PNO group was similar to PSO group. The dominant bacteria in the SBO  
285 group were Proteobacteria, Firmicutes and Bacteroidetes. At the phylum level,  
286 Firmicutes and Bacteroidetes in the treatment group were significantly different from  
287 that in the Con group (Figure 6B;  $P < 0.01$ ,  $P < 0.05$ ,  $P < 0.001$ ).

288 Next, we further analyzed the top 20 taxa at the generic level. As shown in Figure  
289 6C, Lactobacillus, Bacteroides, Prevotella and Prevotella are the dominant bacteria in  
290 the Con group, while the dominant bacteria in the PSO group are Lactobacillus.  
291 Prevotellaceae\_Prevotella, Odoribacter, Allobaculum, etc. The dominant genera in  
292 PNO group and SBO group were Lactobacillus, Allobaculum, Bacteroides and  
293 Bifidobacterium. In addition, as can be seen from the bar chart in Figure 6D, compared  
294 with the Con group, the abundance of Bacteroides, Sutterella, Prevotella and  
295 Parabacteroides in the PSO group was markedly reduced ( $P < 0.01$ ,  $P < 0.001$ ). There  
296 was no significant difference of PNO group in Sutterella, but the bacteria of Bacteroides,  
297 Prevotella and Parabacteroides presented the remarkable difference ( $P < 0.05$ ,  $P <$   
298  $0.001$ ). Moreover, the abundance of Ruminococcaceae\_Ruminococcus, Oscillospira,  
299 Coprococcus, Paraprevotella in PSO group had significant increase compared with Con  
300 group ( $P < 0.01$ ,  $P < 0.05$ ,  $P < 0.001$ ). However, there was no significant difference  
301 of Ruminococcaceae\_Ruminococcus, Coprococcus compared to Con group. Also, the  
302 abundance of Oscillospira, Coprococcus in PNO group had no significant difference.  
303 There findings indicated PSO changed the gut bacterial composition and increased  
304 probiotic abundance to regulate sleep.



305

306 Figure 6 Impact of PSO on gut microbiota composition at the phylum level in Mice. (A)

307 Bar graph illustrating the relative abundance of species at the phylum level (top 20). (B)

308 Species significantly influenced by PSO at the phylum level from the five groups. (C)

309 Bar graph illustrating the relative abundance of species at genus level (top 20). (D)

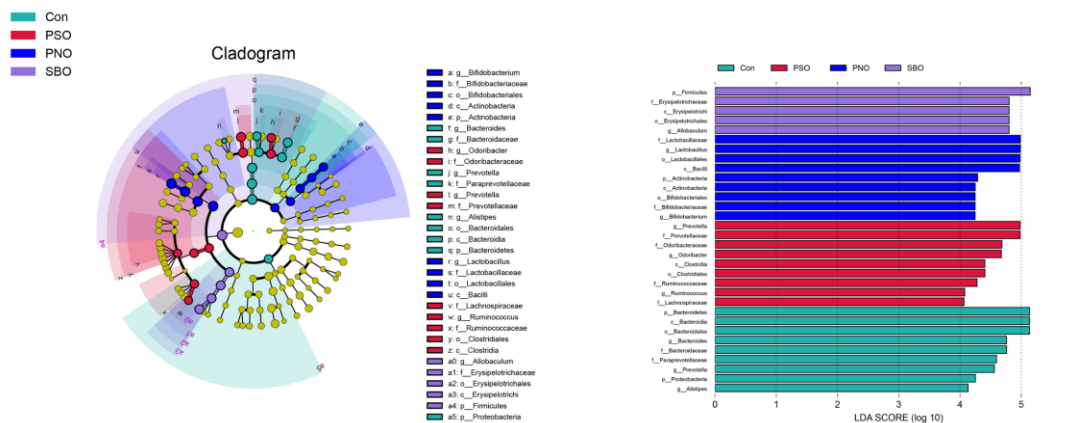
310 Species significantly influenced by PSO at the genus levels from the five groups. \* $P < 0.05$ , \*\* $P < 0.01$ , \*\*\* $P < 0.001$ .

311

312

### 313 3.4.3. Effects of the long-term intake of PSO on fecal microbiota composition and 314 SCFAs

315 The Linear Discriminant Analysis Effect Size (LEfSe) was used to evaluate the effect  
 316 of sample abundance on observed differences ( $P < 0.05$ ,  $LDA > 4.0$ ). The analysis  
 317 results for Con vs PSO, Con vs PNO and Con vs SBO are presented. As shown in Figure  
 318 7, cladogram and LDA scores generated from LEfSe was used to identify biological  
 319 markers with statistical differences in different groups. The Con group exhibited the  
 320 enrichment in Bacteroides, Bacteroidaceae, Prevotella, Prevotella, Paraprevotellaceae,  
 321 Alistipes, Bacteroidales, Bacteroidia, Bacteroidetes. But PSO group was primarily  
 322 enriched in Prevotella, Odoribacter, Ruminococcus, Prevotellaceae Odoribacteraceae,  
 323 Clostridia, Clostridiales, Ruminococcaceae, Lachnospiraceae. The PNO exhibited the  
 324 marker taxa in Bifidobacterium, Bifidobacteriaceae, Bifidobacteriales, Actinobacteria,  
 325 Actinobacteria. Five taxon differences emerged in SBO groups, including Allobaculum,  
 326 Erysipelotrichaceae, Erysipelotrichales, Erysipelotrichi, Firmicutes.

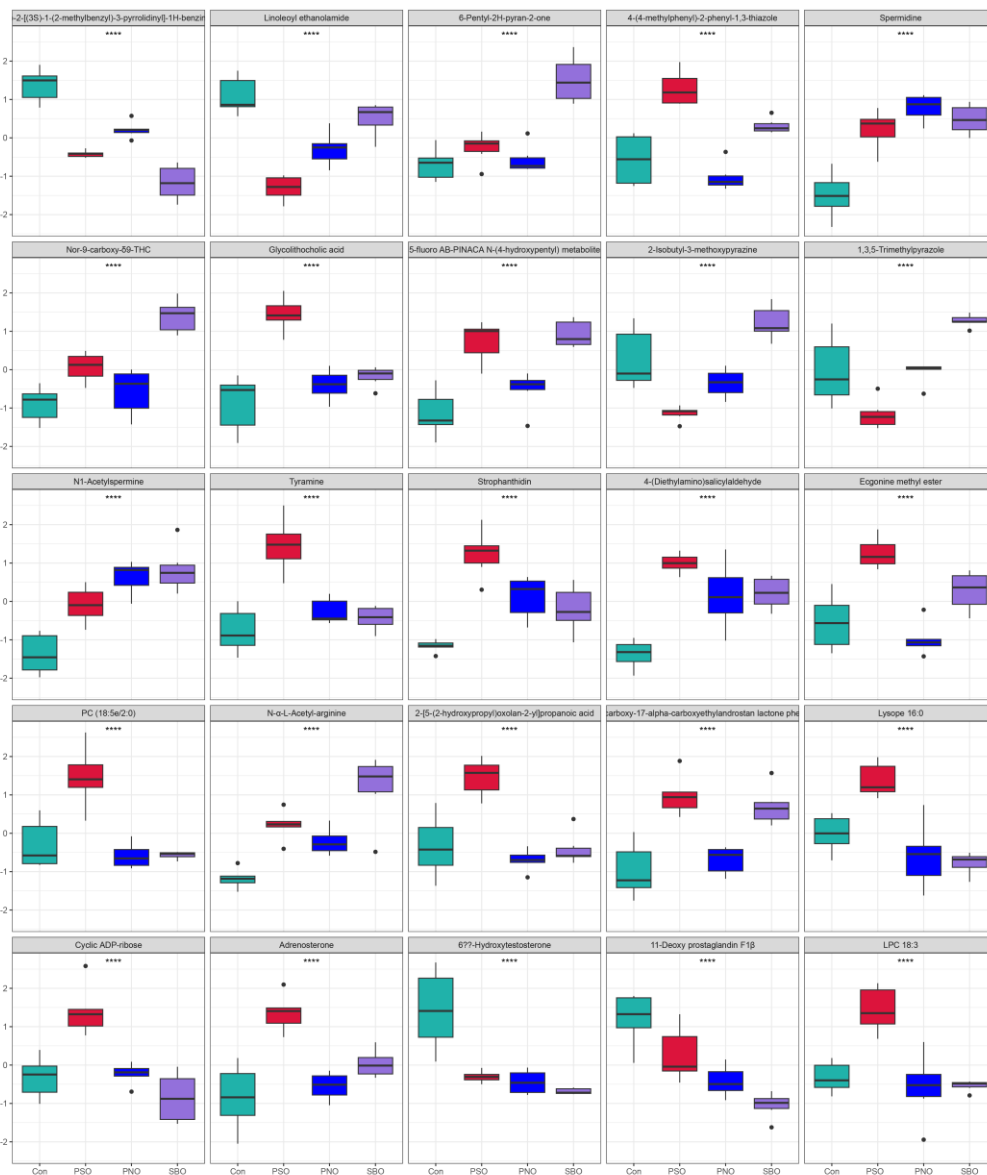


327

328 Figure 7 Significantly different taxonomic biomarkers were identified in different  
 329 groups by LEfSe. The cladogram's circles radiating from the inside out represent the  
 330 classification level from phylum to genus. Taxa without significant differences are  
 331 shown in yellow, while taxa with significant differences are colored based on their  
 332 association with the group exhibiting the highest abundance. Taxa with an LDA score >  
 333 4 are marked as statistically significant and listed on the right side of the figure.

334 Additionally, 2-[5-(2-hydroxypropyl) oxolan 2-yl] propanoic acid is a short-chain

335 fatty acid (SCFA) and the PSO group displayed higher levels of it in box plot compared  
 336 to other 3 groups after 12 weeks of administration (top 25 with lower P values, Figure.  
 337 8).



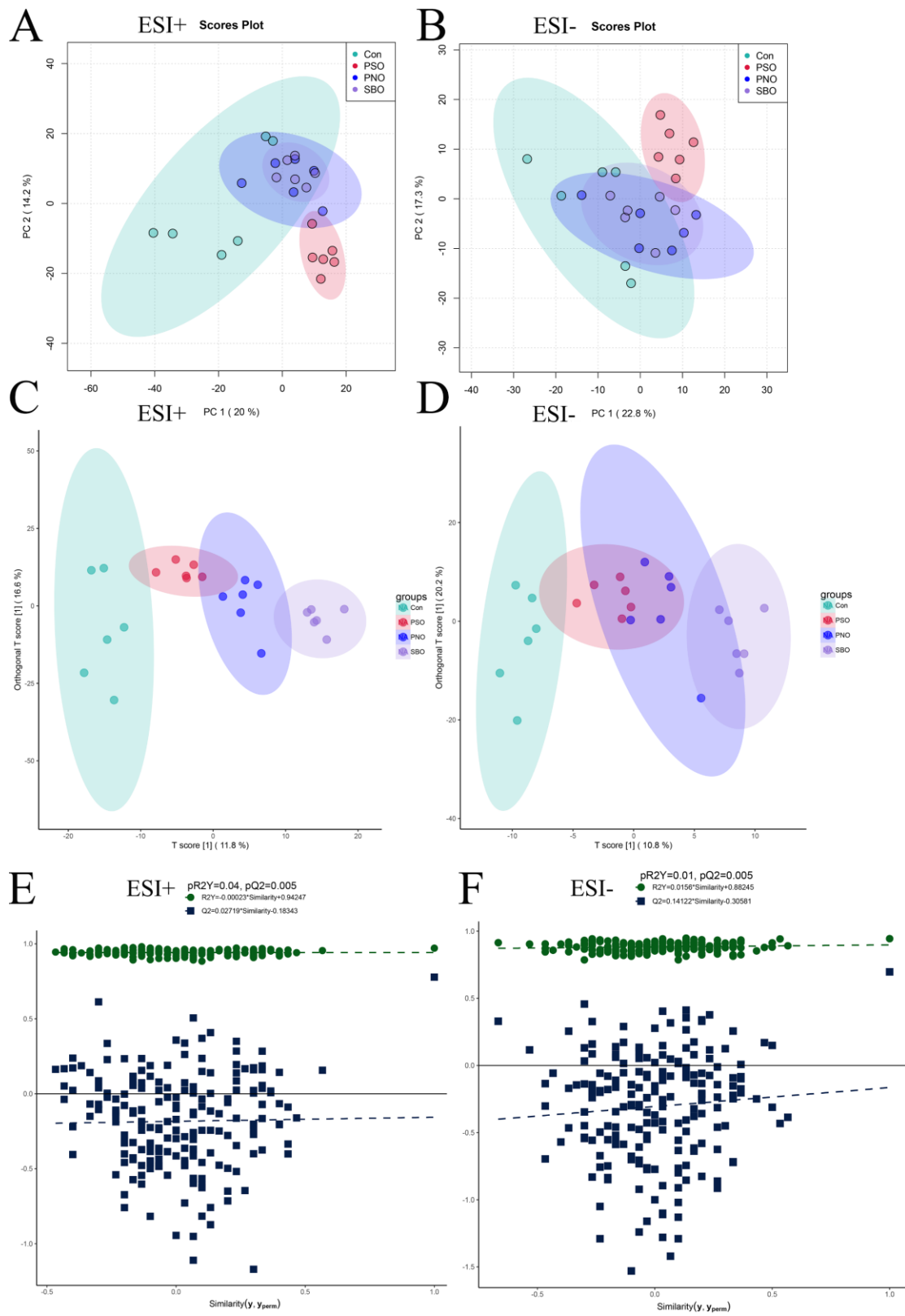
338  
 339 Figure 8 Untargeted metabolomics analysis of SCFAs in positive mode (\*\*\*\*  $P <$   
 340 0.001).

### 341 3.5. Gut metabolome analysis

#### 342 3.5.1. Metabolic profile analysis

343 To further assess the effects of metabolites on mice, we performed untargeted  
 344 metabolomics analysis to detect differences the metabolites in the PSO group, PNO  
 345 group, SBO group and the Con group. The total ion chromatogram (TIC) of the QC

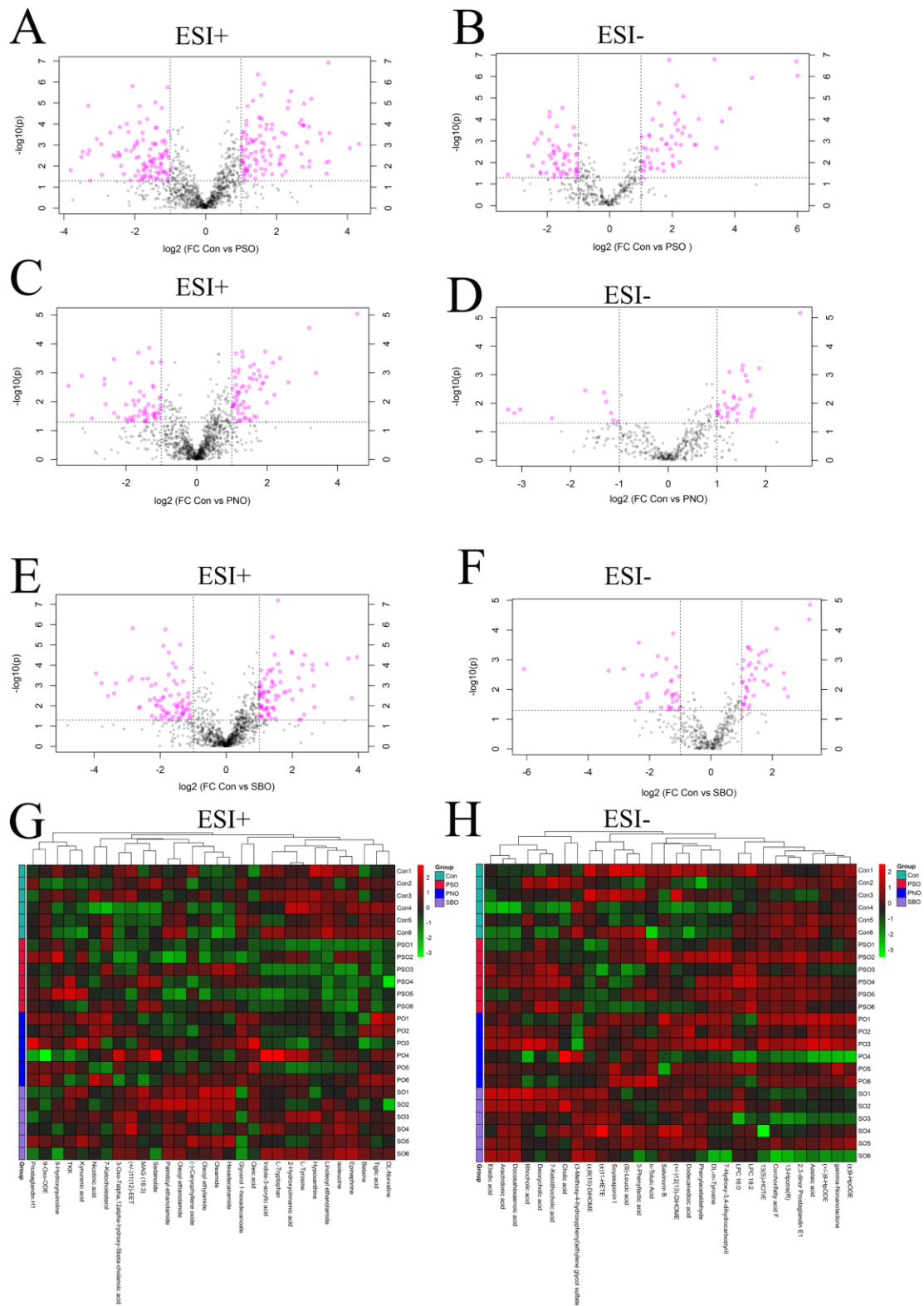
346 samples in both positive and negative ion modes is described in Supplementary Figure  
347 1. The principal components analysis (PCA) scores of positive and negative ions  
348 showed that the blank group was separated from the PSO group, while the Con group,  
349 PNO group and SBO group were cross-aggregated (Figure 9A-B). The OPLS-DA  
350 results of positive and negative ions showed that Con group had significant separation  
351 from PSO group, PNO group and SBO group (Figure 9C-D). The model demonstrated  
352 excellent performance in the positive ion mode, with  $R^2 Y = 0.97$  and  $Q^2 = 0.79$ . In  
353 addition, in the negative ion mode, the model parameters were  $R^2 = 0.94$  and  $Q^2 Y =$   
354  $0.70$ . These values are close to 1, indicating that the model has a high degree of  
355 interpretability and good predictive ability. In the permutation displacement tests of  
356 OPLS-DA,  $pR^2 Y$  and  $pQ^2$  are less than 0.05, which also indicates that the model is  
357 reliable (Figure 9E-F).



358  
 359 Figure 9 Gut metabolomics analysis of serum in both positive and negative ion modes.  
 360 ESI + stands for the positive ion mode, and ESI- stands for the negative ion mode. (A-  
 361 B) PCA analysis score plot. (C-D) OPLS-DA analysis score plot. (E-F) OPLS-DA  
 362 permutation test analysis plot.

### 363 **3.5.2. Analysis of the key metabolites and the metabolic pathways**

364 We use hot maps to identify biomarkers with significant differences ( $P < 0.05$ ,  
365  $|\log_2FC| > 2$ ). We only focus on the top 10 most significant metabolite names  
366 (Supplementary Table 2). In positive mode of Con vs PSO, according to HMDB  
367 classification, upregulate metabolite included TMK, 3-[(4-hydroxyphenyl)methyl]-  
368 octahydropyrrolo[1,2-a]pyrazine-1,4-dione, (Diethylamino) salicylaldehyde,  
369 Spermidine, PC (18:4e/2:0), PC (18:5e/2:0). Downregulate metabolite mainly was  
370 Linoleoyl ethanolamide, 5-Fluoro-2-[(3S)-1-(2-methylbenzyl)-3-pyrrolidinyl]-1H-  
371 benzimidazole, Folinic acid, Pinocembrin, 1,3,5-Trimethylpyrazole (Figure 10A). In  
372 negative mode of Con vs PSO, upregulate metabolite comprised tetranor-PGFM,  
373 Epicatechin, Catechin, N'-(4-chlorophenyl)-4-ethylbenzohydrazide, 5-Phenylvaleric  
374 Acid, Phloretin, D-(-)-Mannitol, cis-Aconitic acid (Figure 10B). In positive mode of  
375 Con vs PNO, 4 belonged to others. 2 belonged to lipids and lipid-like molecules. 2  
376 belonged to organic acids and derivatives. 2 belonged to phenylpropanoids and  
377 polyketides (Figure 10C). In negative mode of Con vs PNO, 5 belonged to others. 2  
378 belonged to lipids and lipid-like molecules. 1 belonged to organic acids and derivatives.  
379 1 belonged to organoheterocyclic compounds. 2 belonged to nucleosides, nucleotides,  
380 and analogues (Figure 10D). In positive mode of Con vs SBO, 2 belonged to organic  
381 acids and derivatives. 6 belonged to others. 1 belonged to organic nitrogen compounds.  
382 2 belonged to lipids and lipid-like molecules. 2 belonged to phenylpropanoids and  
383 polyketides (Figure 10E). In negative mode of Con vs SBO, 3 belonged to others. 1  
384 belonged to benzenoids. 2 belonged to lipids and lipid-like molecules. 1 belonged to  
385 organic acids and derivatives. 2 belonged to nucleosides, nucleotides, and analogues. 1  
386 belonged to organoheterocyclic compounds (Figure 10F). The difference of metabolites  
387 in different treatment groups was further analyzed by heat map analysis, and the results  
388 showed that the composition and structure of these 30 metabolites were significantly  
389 different among different groups (Figure 10G-H).



390

391 Figure 10 Effects of PSO on intestinal metabolites. (A-B) Volcano plot of Con vs PSO

392 in positive mode and negative mode. (C-D) Volcano plot of Con vs PNO in positive

393 mode and negative mode. (E-F) Volcano plot of Con vs SBO in positive mode and

394 negative mode. (G-H) Heatmap of the top 30 metabolites of 4 groups in positive mode

395 negative mode.

396 We perform metabolic analysis by KEGG and calculate the ORA (Over-  
397 Representation Analysis) *P*-values of these metabolic pathways to determine whether  
398 the metabolites of interest are significantly enriched in these metabolic pathways. In  
399 positive mode of Con vs PSO, significant enriched metabolic pathways were nucleotide  
400 metabolism, steroid hormone biosynthesis, vitamin B6 metabolism (Figure 11A). In  
401 negative mode, Figure 11A showed that the chosen biomarkers are highly involved in  
402 the pathway network related to TCA cycle, alanine, aspartate and glutamate metabolism,  
403 arginine biosynthesis, glyoxylate and dicarboxylate metabolism and so on. The result  
404 indicated that sleep may be connected with these multiple pathways and the potential  
405 role of PSO in regulating sleep by influencing key metabolites and the aforementioned  
406 metabolic pathways. In positive mode of Con vs PNO (Figure 11C), obvious enriched  
407 metabolic pathways were nucleotide metabolism, vitamin B6 metabolism,  
408 phenylalanine metabolism, purine metabolism, arginine and proline metabolism. In  
409 negative mode, PNO regulated the Biosynthesis of unsaturated fatty acids, linoleic acid  
410 metabolism, and nucleotide metabolism pathway (Figure 11D). In positive mode of Con  
411 vs SBO (Figure 11E), the remarkable enriched metabolic pathways only were steroid  
412 hormone biosynthesis, nucleotide metabolism. And SBO group adjusted 5 pathways in  
413 negative mode (Figure 11F).

414

415

416

417

418

419

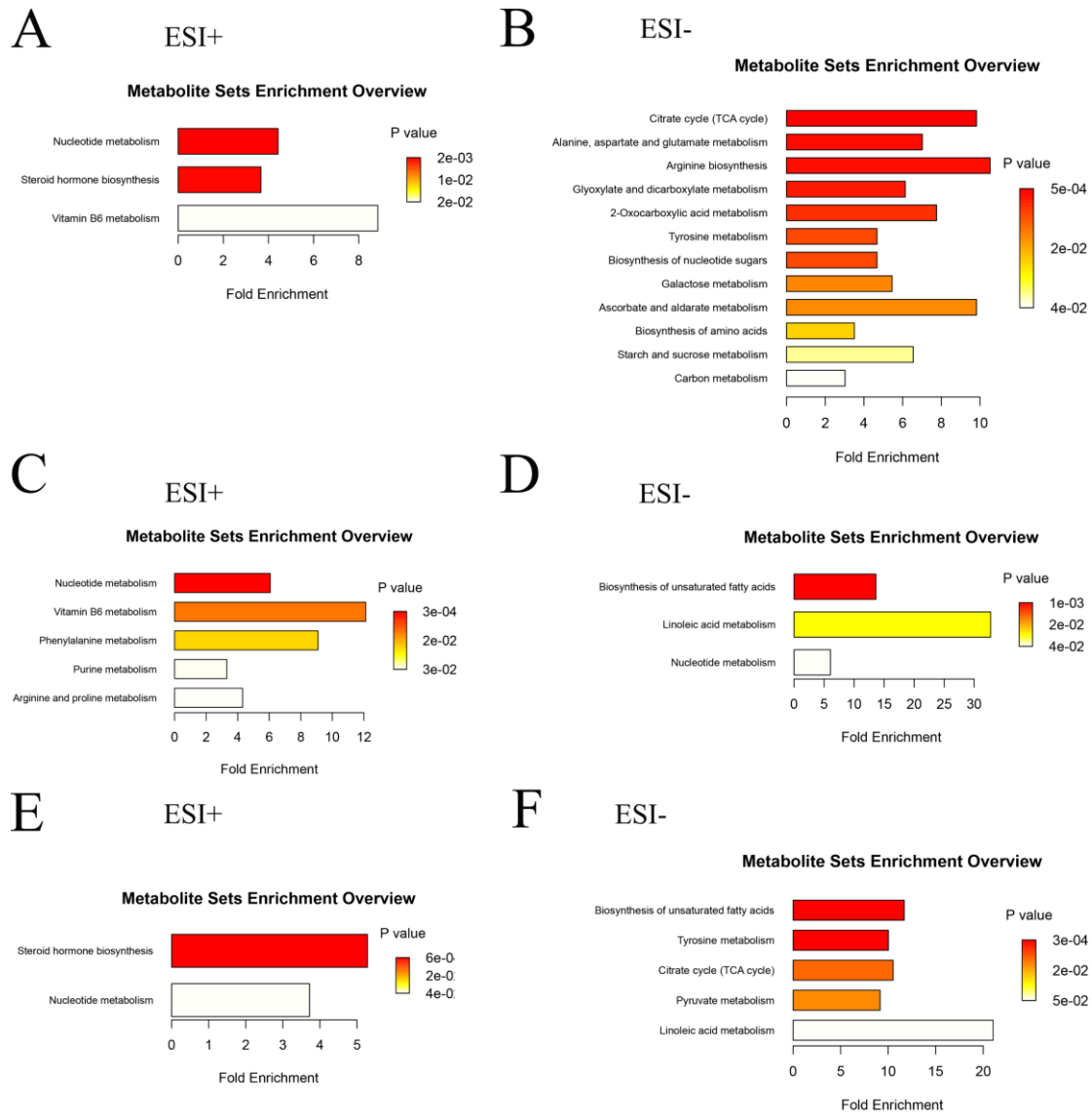
420

421

422

423

424



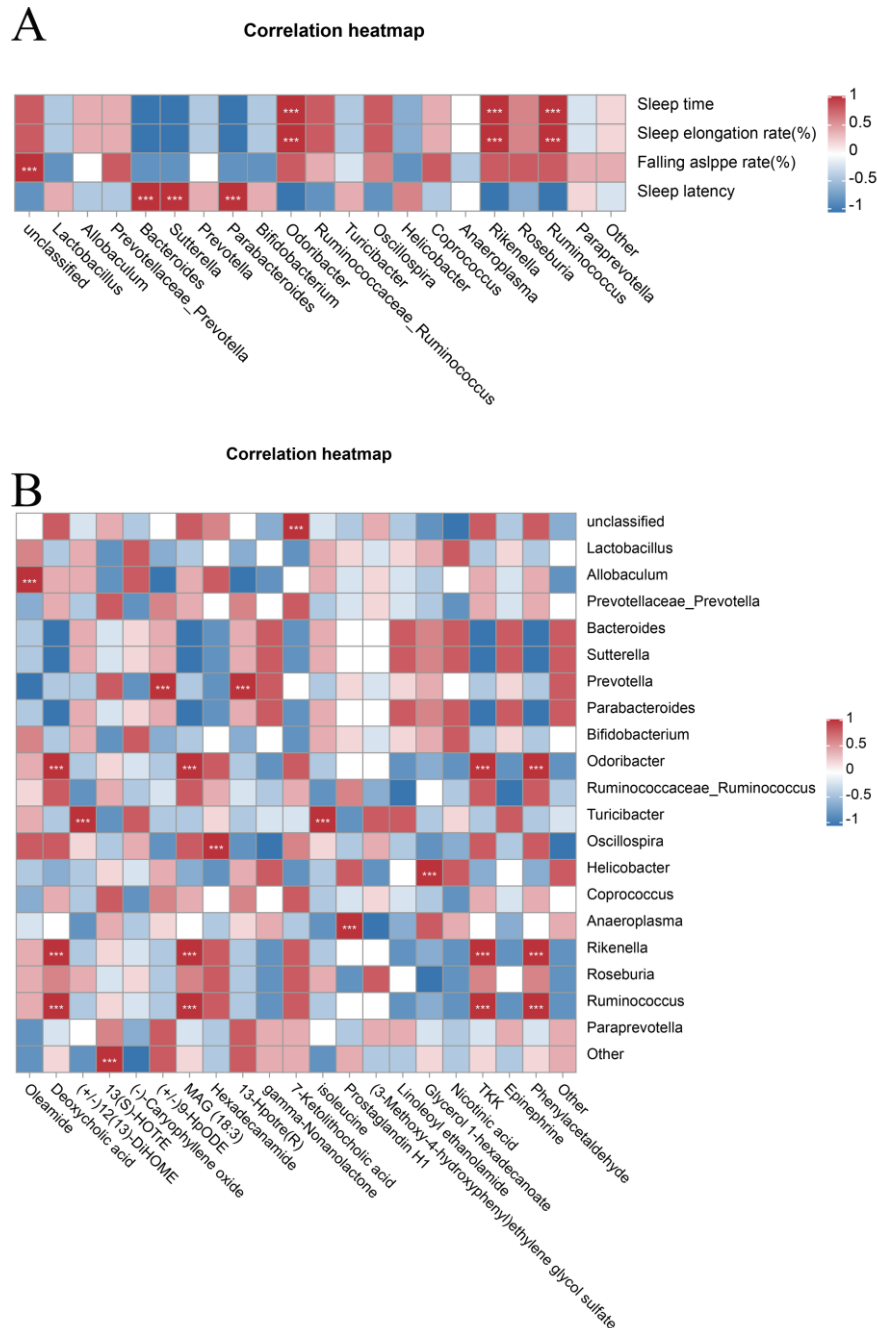
425

426 Figure 11 KEGG metabolic pathway enrichment analysis of Con vs PSO in positive  
 427 mode (A) and negative mode (B). KEGG metabolic enrichment analysis of Con vs PNO  
 428 in positive mode (C) and negative mode (D). KEGG metabolic enrichment analysis of  
 429 Con vs SBO in positive mode (E) and negative mode (F). ( $P < 0.05$ )

### 430 3.6. Integration analysis

431 In order to further explore the relationship among sleep, gut microbes and  
 432 metabolites, we executed the correlation analysis using Spearman's analysis method.  
 433 The study performed a correlation matrix linking the top 20 bacteria with the  
 434 aforementioned 4 sleep indexes. Both sleep time and sleep elongation rate were  
 435 positively related to *Odoribacter*, *Rikenella* and *Ruminococcus* (Figure 12A,  $P < 0.001$ ).  
 436 Sleep latency had a positive correlated with *Bacterioides*, *Sutterella* and

437 Parabacteriodes ( $P < 0.001$ ). The association analysis of top 20 bacteria and metabolites  
 438 found that 11 bacteria were positively correlated with 13 metabolites (Figure 12B,  $P <$   
 439  $0.001$ ). These descriptions manifested that gut microbiota and gut metabolites played  
 440 an essential role in regulating sleep.  
 441



442  
 443 Figure 12 (A) Correlation heatmap between differential genus-level bacteria and sleep  
 444 indicators. (B) Correlation heatmap between differential genus-level bacteria and  
 445 differential metabolites (positive and negative ion combined) analysis. \*\*\* $P < 0.001$ .

#### 446 **4. Discussion**

447 In our study found the PSO had a lot of unsaturated fatty acid, which was up to 90%.  
448 Rish unsaturated fatty acid was considered to have the effect of improving sleep  
449 quality<sup>[14]</sup>. In addition, in terms of physiological indexes such as TG, TC, LDL-C, HDL-  
450 C and Glu, as well as liver H&E staining indexes, the results of PSO and other edible  
451 oils were not significantly different, indicating that PSO had good safety. Many  
452 previous articles have focused on alleviating hyperlipidemia and hyperglycemia or anti-  
453 obesity on gut microbiome and untargeted metabolomics<sup>[15-17]</sup>. However, In this study,  
454 It is the first time that we analysed the sleep principle of PSO from the perspective of  
455 gut microbes and untargeted metabolomics.

456 In our experiment, PSO group could prolong sleep time and reduce sleep latency.  
457 Some studies have shown that 5-hydroxytryptamine (5-HT) and  $\gamma$ -aminobutyric acid  
458 (GABA) are involved in sleep regulation<sup>[18,19]</sup>. Reports indicate that therapeutic drugs  
459 cause sedation and hypnosis by modulating neurotransmission pathways, including the  
460 5-HT and GABA systems within the central nervous system<sup>[20]</sup>. 5-HT regulates sleep  
461 by eventually converting into melatonin<sup>[21]</sup>. But GABA binds to receptors on neurons,  
462 it can inhibit the firing frequency of neurons, resulting in sedation and sleep<sup>[22]</sup>. It has  
463 been reported that some components of vegetable oil could promote sleep by elevating  
464 5-HT level and enhance GABA synthesis to promote GABA A receptor to express<sup>[23]</sup>.  
465 Our study adds valuable evidence and reveals new links between PSO and  
466 neurotransmitters in sleep.

467 It has been reported that the gut microbiome is a source of signals that promote  
468 sleep<sup>[24]</sup>. Microbiome diversity and abundance ( $\alpha$  and  $\beta$  diversity) are positively  
469 correlated with improved sleep quality and increased total sleep duration.<sup>[25]</sup> Our  
470 experimental results show that the PSO group increased gut richness and diversity in  
471 mice. Previous study showed that the abundance of Bacteroidetes and Firmicutes has  
472 positive correlation with sleep quality<sup>[26]</sup>. A higher proportion of Verrucomicrobia is  
473 associated with improved cognitive function<sup>[27]</sup>. In our experiment, the abundances of  
474 Bacteroidetes, Firmicutes, and Verrucomicrobia were relatively high. *Lactobacillus* spp.  
475 regulates sleep disorders and memory by converting the excitatory neurotransmitter

476 glutamate into the primary inhibitory neurotransmitter GABA through the GABAergic  
477 receptor system<sup>[28]</sup>. Studies have reported that the gut microbiome induces non-rapid  
478 eye movement sleep through a butyrate-sensitive mechanism<sup>[29]</sup>. In PSO group, bacteria  
479 such as *Oscillibacter*, *Ruminococcus*, *Allobaculum*, *Lachnospiraceae*, can participate in  
480 butyrate production, which is consistent with previous research findings<sup>[30]</sup>.

481 Bacterial metabolites may provide a crucial link between gut symbiotic  
482 communities and sleep-generating mechanisms in the brain. Some studies suggest that  
483 a higher proportion of fecal SCFA propionate is associated with longer periods of  
484 uninterrupted sleep<sup>[31,32]</sup>. And propionic acid has the ability to influence  
485 neurotransmitter concentrations, such as glutamate, GABA, and tryptophan, thereby  
486 affecting emotional regulation, cognitive functions, and behavioral patterns<sup>[33]</sup>. In our  
487 experiment, the propionate content in the PSO group was higher than that in other  
488 groups. Our untargeted metabolomics results indicate that the PSO group is involved in  
489 vitamin B6 metabolism, glutamate metabolism and arginine biosynthesis. Vitamin B6  
490 plays a vital role in the synthesis of several neurotransmitters, including serotonin and  
491 GABA, which are critical for promoting sleep<sup>[34]</sup>. Glutamate is the precursor of GABA  
492 and maintains a balance with it<sup>[35]</sup>. Arginine is converted into nitric oxide in the body,  
493 which promotes blood circulation and relaxes blood vessels, potentially aiding in  
494 improving sleep quality<sup>[36]</sup>.

495 In summary, the regulatory mechanism of PSO was investigated in an animal model  
496 using metabolomics and gut microbiota analysis. After gavaging with PSO, there were  
497 no differences in liver levels and blood markers in mice compared to other edible oils.  
498 The mice showed improved sleep quality, increased sleep duration, and decreased sleep  
499 latency. PSO significantly altered the gut microbiota of the mice, increasing the  
500 abundance of short-chain fatty acids and promoting the production of sleep-promoting  
501 metabolites. Further research is necessary to comprehensively understand the precise  
502 regulatory mechanisms underlying the influence of PSO.

503

504

505 **Data Availability Statement**

506 The data presented in this study are available on request from the corresponding  
507 author. Data sets generated and/or analyzed in the current study are available in  
508 supplementary information.

509 **Support information**

510 Supporting information may be found in the online version of this article.

511 **Conflicts of interest statement**

512 The authors have no conflicts of interest.

513

514 [1] Announcement: Sleep Awareness Week - March 6-12, 2016[J].MMWR Morb Mortal Wkly  
515 Rep,2016, 65 (8): 217.

516 [2] Stein M B, Belik S L, Jacobi F, et al.Impairment associated with sleep problems in the community:  
517 relationship to physical and mental health comorbidity[J].Psychosom Med,2008, 70 (8): 913-9.

518 [3] Parati G, Lombardi C, Castagna F, et al.Heart failure and sleep disorders[J].Nat Rev Cardiol,2016,  
519 13 (7): 389-403.

520 [4] Gao X, Su X, Han X, et al.Unsaturated Fatty Acids in Mental Disorders: An Umbrella Review of  
521 Meta-Analyses[J].Adv Nutr,2022, 13 (6): 2217-2236.

522 [5] Petersen K S, Maki K C, Calder P C, et al.Perspective on the health effects of unsaturated fatty  
523 acids and commonly consumed plant oils high in unsaturated fat[J].Br J Nutr,2024: 1-12.

524 [6] Akbarzadeh S S, Pourfakhraei E, Zargar M, et al.Introducing of high rich lysine, arginine, and  
525 unsaturated fatty acids microalga as a food supplement[J].World J Microbiol Biotechnol,2023, 40  
526 (2): 43.

527 [7] Yang Y, Ge S, Chen Q, et al.Chlorella unsaturated fatty acids suppress high-fat diet-induced  
528 obesity in C57/BL6J mice[J].J Food Sci,2022, 87 (8): 3644-3658.

529 [8] Wang Z, Wang Z, Lu T, et al.The microbiota-gut-brain axis in sleep disorders[J].Sleep Med  
530 Rev,2022, 65: 101691.

531 [9] Anderson J R, Carroll I, Azcarate-Peril M A, et al.A preliminary examination of gut microbiota,  
532 sleep, and cognitive flexibility in healthy older adults[J].Sleep Med,2017, 38: 104-107.

533 [10] Poroyko V A, Carreras A, Khalyfa A, et al.Chronic Sleep Disruption Alters Gut Microbiota,  
534 Induces Systemic and Adipose Tissue Inflammation and Insulin Resistance in Mice[J].Sci Rep,2016,  
535 6: 35405.

536 [11] He W S, Wang Q, Zhao L, et al.Nutritional composition, health-promoting effects,  
537 bioavailability, and encapsulation of tree peony seed oil: a review[J].Food Funct,2023, 14 (23):  
538 10265-10285.

539 [12] Meng J S, Tang Y H, Sun J, et al.Identification of genes associated with the biosynthesis of  
540 unsaturated fatty acid and oil accumulation in herbaceous peony 'Hangshao' (Paeonia lactiflora  
541 'Hangshao') seeds based on transcriptome analysis[J].BMC Genomics,2021, 22 (1): 94.

542 [13] Liang Z, He Y, Wei D, et al.Tree peony seed oil alleviates hyperlipidemia and hyperglycemia

543 by modulating gut microbiota and metabolites in high-fat diet mice[J].*Food Sci Nutr*,2024, 12 (6):  
544 4421-4434.

545 [14] Iqbal A Z, Wu S K, Zailani H, et al.Effects of Omega-3 Polyunsaturated Fatty Acids Intake on  
546 Vasomotor Symptoms, Sleep Quality and Depression in Postmenopausal Women: A Systematic  
547 Review[J].*Nutrients*,2023, 15 (19).

548 [15] He W S, Wang Q, Zhao L, et al.Nutritional composition, health-promoting effects,  
549 bioavailability, and encapsulation of tree peony seed oil: a review[J].*Food Funct*,2023, 14 (23):  
550 10265-10285.

551 [16] Kwek E, Zhu H, Ding H, et al.Peony seed oil decreases plasma cholesterol and favorably  
552 modulates gut microbiota in hypercholesterolemic hamsters[J].*Eur J Nutr*,2022, 61 (5): 2341-2356.

553 [17] Liang Z, He Y, Wei D, et al.Tree peony seed oil alleviates hyperlipidemia and hyperglycemia  
554 by modulating gut microbiota and metabolites in high-fat diet mice[J].*Food Sci Nutr*,2024, 12 (6):  
555 4421-4434.

556 [18] Xu P, Huang S, Zhang H, et al.Structural insights into the lipid and ligand regulation of  
557 serotonin receptors[J].*Nature*,2021, 592 (7854): 469-473.

558 [19] Hepsomali P, Groeger J A, Nishihira J, et al.Effects of Oral Gamma-Aminobutyric Acid (GABA)  
559 Administration on Stress and Sleep in Humans: A Systematic Review[J].*Front Neurosci*,2020, 14:  
560 923.

561 [20] Zhong Y, Zheng Q, Hu P, et al.Sedative and hypnotic effects of compound Anshen essential  
562 oil inhalation for insomnia[J].*BMC Complement Altern Med*,2019, 19 (1): 306.

563 [21] Stauch B, Johansson L C, Mccorvy J D, et al.Structural basis of ligand recognition at the human  
564 MT(1) melatonin receptor[J].*Nature*,2019, 569 (7755): 284-288.

565 [22] Thompson S M.Modulators of GABA(A) receptor-mediated inhibition in the treatment of  
566 neuropsychiatric disorders: past, present, and future[J].*Neuropsychopharmacology*,2024, 49 (1):  
567 83-95.

568 [23] Sun M, Li M, Cui X, et al.Terpenoids derived from Semen Ziziphi Spinosae oil enhance sleep  
569 by modulating neurotransmitter signaling in mice[J].*Heliyon*,2024, 10 (5): e26979.

570 [24] Wang Z, Wang Z, Lu T, et al.The microbiota-gut-brain axis in sleep disorders[J].*Sleep Med*  
571 *Rev*,2022, 65: 101691.

572 [25] Wang Z, Chen W H, Li S X, et al.Gut microbiota modulates the inflammatory response and  
573 cognitive impairment induced by sleep deprivation[J].*Mol Psychiatry*,2021, 26 (11): 6277-6292.

574 [26] Grosicki G J, Riemann B L, Flatt A A, et al.Self-reported sleep quality is associated with gut  
575 microbiome composition in young, healthy individuals: a pilot study[J].*Sleep Med*,2020, 73: 76-81.

576 [27] Anderson J R, Carroll I, Azcarate-Peril M A, et al.A preliminary examination of gut microbiota,  
577 sleep, and cognitive flexibility in healthy older adults[J].*Sleep Med*,2017, 38: 104-107.

578 [28] Diez-Gutiérrez L, San Vicente L, R. Barrón L J, et al.Gamma-aminobutyric acid and probiotics:  
579 Multiple health benefits and their future in the global functional food and nutraceuticals  
580 market[J].*Journal of Functional Foods*,2020, 64: 103669.

581 [29] Grosicki G J, Riemann B L, Flatt A A, et al.Self-reported sleep quality is associated with gut  
582 microbiome composition in young, healthy individuals: a pilot study[J].*Sleep Med*,2020, 73: 76-81.

583 [30] Wu J, Zhang B, Zhou S, et al.Associations between gut microbiota and sleep: a two-sample,  
584 bidirectional Mendelian randomization study[J].*Front Microbiol*,2023, 14: 1236847.

585 [31] Magzal F, Even C, Haimov I, et al.Associations between fecal short-chain fatty acids and sleep  
586 continuity in older adults with insomnia symptoms[J].*Sci Rep*,2021, 11 (1): 4052.

- 587 [32] Heath A M, Haszard J J, Galland B C, et al. Association between the faecal short-chain fatty  
588 acid propionate and infant sleep[J]. *Eur J Clin Nutr*, 2020, 74 (9): 1362-1365.
- 589 [33] Decastro M, Nankova B B, Shah P, et al. Short chain fatty acids regulate tyrosine hydroxylase  
590 gene expression through a cAMP-dependent signaling pathway[J]. *Brain Res Mol Brain Res*, 2005,  
591 142 (1): 28-38.
- 592 [34] Ge L, Luo J, Zhang L, et al. Association of Pyridoxal 5'-Phosphate with Sleep-Related Problems  
593 in a General Population[J]. *Nutrients*, 2022, 14 (17).
- 594 [35] Albarracin S L, Baldeon M E, Sangronis E, et al. L-glutamate: a key amino acid for sensory and  
595 metabolic functions[J]. *Arch Latinoam Nutr*, 2016, 66 (2): 101-112.
- 596 [36] Jiang J, Gan Z, Li Y, et al. REM sleep deprivation induces endothelial dysfunction and  
597 hypertension in middle-aged rats: Roles of the eNOS/NO/cGMP pathway and supplementation  
598 with L-arginine[J]. *PLoS One*, 2017, 12 (8): e0182746.
- 599